Development 135, 2555-2562 (2008) doi:10.1242/dev.019877

Mesp2 and Tbx6 cooperatively create periodic patterns coupled with the clock machinery during mouse somitogenesis

Masayuki Oginuma[1], Yasutaka Niwa[2], Deborah L. Chapman[3] and Yumiko Saga[1,4,*]

The metameric structures in vertebrates are based on the periodicity of the somites that are formed one by one from the anterior end of the presomitic mesoderm (PSM). The timing and spacing of somitogenesis are regulated by the segmentation clock, which is characterized by the oscillation of several signaling pathways in mice. The temporal information needs to be translated into a spatial pattern in the so-called determination front, at which cells become responsive to the clock signal. The transcription factor Mesp2 plays a crucial role in this process, regulating segmental border formation and rostro-caudal patterning. However, the mechanisms regulating the spatially restricted and periodic expression of *Mesp2* have remained elusive. Using high-resolution fluorescent in situ hybridization in conjunction with immunohistochemical analyses, we have found a clear link between *Mesp2* transcription and the periodic waves of Notch activity. We also find that *Mesp2* transcription is spatially defined by Tbx6: *Mesp2* transcription and Tbx6 protein initially share an identical anterior border in the PSM, but once translated, Mesp2 protein leads to the suppression of Tbx6 protein expression post-translationally via rapid degradation mediated by the ubiquitin-proteasome pathway. This reciprocal regulation is the spatial mechanism that successively defines the position of the next anterior border of *Mesp2*. We further show that FGF signaling provides a spatial cue to position the expression domain of *Mesp2*. Taken together, we conclude that Mesp2 is the final output signal by which the temporal information from the segmentation clock is translated into segmental patterning during mouse somitogenesis.

KEY WORDS: Notch signaling, Tbx6, Segmentation clock, Presomitic mesoderm, Mouse

INTRODUCTION

Elaborate somite patterning is based upon dynamic gene regulation within the presomitic mesoderm (PSM), which is derived from the primitive streak and tailbud in the later stage mouse embryo. The Notch signaling pathway and its regulators are major components of most of the events required for temporally and spatially coordinated somite formation. In the posterior PSM, oscillations of Notch activity and the bHLH protein Hes7 play central roles as so-called segmentation clock components in generating traveling waves of gene expression by either positively or negatively regulating the transcription of their target genes (Bessho et al., 2003; Bessho et al., 2001; Huppert et al., 2005). In the anterior PSM, Notch activity is stabilized and cells begin to form segmental pattern by acquiring rostral or caudal identities of somite primordia and by defining the segmental border (Morimoto et al., 2005).

Our previous studies demonstrated that the transcription factor Mesp2 is expressed periodically in the anterior PSM and that this is required for both segmental border formation and the establishment of rostro-caudal (RC) patterning within a somite (Morimoto et al., 2005; Takahashi et al., 2000). The segmentation boundary is defined by the so-called determination front, which is thought to be defined by an antagonistic gradient of retinoic acid (RA) and FGF signaling (Delfini et al., 2005; Moreno and Kintner, 2004; Wahl et al., 2007). Although the *Mesp2* expression domain appears to be defined by a determination front, we previously showed that the *Mesp2* expression domain was not affected when RA signaling was upregulated by inactivation of Cyp26a1 in the posterior PSM (Morimoto et al., 2005). Furthermore, the role of FGF signaling remains controversial because both positive and negative effects of this signaling upon *Mesp2* expression have been reported (Delfini et al., 2005; Wahl et al., 2007). Recently, it was also reported that Wnt signaling functions upstream of FGF signaling to maintain the immature property of PSM cells, indicating the involvement of Wnt signaling in regulating *Mesp2* expression (Aulehla et al., 2007; Dunty et al., 2008).

The temporal information provided by the segmentation clock needs to be translated into a spatial pattern in the anterior PSM. Therefore, the link between the clock and segmental border formation is of fundamental importance during somitogenesis. We have previously shown that Mesp2 functions to mediate this translation in the anterior PSM and that *Mesp2* expression is positively regulated by Notch and Tbx6 (Yasuhiko et al., 2006). However, the mechanisms involved in the spatially restricted and periodic expression of *Mesp2* have remained elusive. Accurate analyses of spatio-temporal relationships among several factors are particularly difficult because somitogenesis is a dynamic and periodic process, in which the associated gene activities also change periodically in a cycle of 2 hours. To overcome this difficulty, we have employed high-resolution fluorescent in situ hybridization in conjunction with immunohistochemical staining of sections derived from single specimens, and this has enabled us to investigate regulatory networks operating in the process of somitogenesis. Finally, we defined the spatio-temporal relationships among *Mesp2* transcription, Mesp2 protein expression, Notch activity state and Tbx6 expression in the anterior end of the PSM, and found that these

[1]Department of Genetics, SOKENDAI, 1111 Yata, Mishima, Shizuoka 411-8540, Japan. [2]Institute for Virus Research, Kyoto University, Kyoto 606-8507, Japan. [3]Department of Biological Sciences, University of Pittsburgh, Pittsburgh, Pennsylvania, PA 15260, USA. [4]Division of Mammalian Development, National Institute of Genetics, Yata 1111, Mishima 411-8540, Japan.

*Author for correspondence (e-mail: ysaga@lab.nig.ac.jp)

Accepted 27 May 2008

factors are dynamically regulated not only at the transcriptional level, but also at the post-translational level, which led us to propose a model for generating periodicity in somitogenesis.

MATERIALS AND METHODS

Animals

The wild-type mice used in this study are MCH (a closed colony established at CLEA, Japan). The *Mesp2*-null mouse (*Mesp2-lacZ* knock-in mouse) was maintained in the animal facility of the National Institute of Genetics, Japan (Takahashi et al., 2000). The conditional *Fgfr1* knockout mouse was generated by crossing an *Fgfr1* floxed mouse with a *Hes7-Cre* mouse and the embryos were recovered at E9.5-10.5 (Niwa et al., 2007; Xu et al., 2002). Noon on the day of the copulation plug was defined as embryonic day (E) 0.5.

Whole-mount in situ hybridization and immunohistochemistry

The InsituPro system (M&S Instruments) was used for whole-mount in situ hybridization according to the manufacturer's instructions. Probes were prepared as described previously: *Mesp2* (Takahashi et al., 2000), *Tbx6* (Yasuhiko et al., 2006) and *Dusp4* (Niwa et al., 2007). The *Msgn1* cRNA probe was prepared against PCR-amplified *Msgn1* exon 1. Whole-mount immunohistochemistry was performed using an anti-Tbx6 antibody as described previously (White and Chapman, 2005).

Explant culture experiments with inhibitors

The caudal part of E10 mouse embryos was bisected along the midline. The explants were cultured in DMEM (Gibco) supplemented with 20% fetal bovine serum with or without inhibitors 100 μM SU5402 (Calbiochem), 50 μM MG132 or 1 mM PMSF, at 37°C for 2 or 6 hours.

Section in situ hybridization and immunohistochemistry

Mouse embryo and tail samples were fixed in 4% paraformaldehyde (PFA), embedded in OCT compound and frozen in liquid nitrogen. For double in situ hybridizations, frozen sections (8 μm) were hybridized with digoxigenin (DIG)-labeled antisense cRNA probes for *Dusp4* and biotin-labeled antisense cRNA probes for *Mesp2*. Hybridized DIG-probes were detected using a horseradish peroxidase-conjugated anti-DIG sheep antibody (Roche) and Cyanin 3 tyramid (Perkin Elmer) signal detection. Hybridized biotin-probes were detected using horseradish peroxidase-conjugated streptavidin (Roche) and fluorescein isothiocyanate-conjugated tyramid (Perkin Elmer) signal detection. For double immunohistochemistry, frozen sections (8 μm) were immersed in unmasking solution (Vector Laboratories) and autoclaved at 105°C for 15 minutes to enable antigen retrieval. Antibody reactions and the detection of Notch1 activity, Mesp2 and Tbx6 were separately conducted after antigen retrieval. The detection of Notch1 activity or Mesp2 was performed by incubation with anti-active-NICD (1:200, Cell Signaling Technology) or anti-Mesp2 (1:400) primary antibodies, respectively, followed by incubation with horseradish peroxidase-conjugated donkey anti-rabbit IgG antibody (1:200, Amersham Pharmacia Biotech) and treatment with Cyanin 3 tyramid. For the detection of Mesp2 or Tbx6, anti-Mesp2 (1:400) or anti-Tbx6 (1:1000) horseradish peroxidase-conjugated donkey anti-rabbit IgG antibodies (1:400, Amersham Pharmacia Biotech) were used, respectively, followed by fluorescein isothiocyanate-conjugated tyramid signal detection.

For double staining by immunohistochemistry and *Mesp2* in situ hybridization, frozen sections (8 μm) were immersed in unmasking solution (Vector Laboratories) and autoclaved at 105°C for 15 minutes to enable antigen retrieval. Notch1 activity and Tbx6 were detected by incubation with anti-active-NICD (1:200) or anti-Tbx6 (1:1000) primary antibodies, followed by a biotinylated goat anti-rabbit IgG secondary antibody (1:200, Vector Laboratories). These sections were then hybridized with a DIG-labeled antisense *Mesp2* cRNA probe. To increase sensitivity, separate cRNA probes were prepared against PCR-amplified *Mesp2* exon 1, intron 1 or exon 2 and used as a mixture. The hybridized probes were detected using horseradish peroxidase-conjugated anti-DIG sheep antibodies and Cyanin 3 tyramid signal detection. Notch1 activity and Tbx6 were detected using horseradish peroxidase-conjugated streptavidin and fluorescein isothiocyanate-conjugated tyramid signal detection. Each section was occasionally counterstained with 0.5 μg/ml 4′-6-diamino-2-phenylindole (DAPI) for 10 minutes and examined using an Olympus BX61 fluorescence microscope system with an ORCA-ER digital camera (Hamamatsu Photo). Subsequent analysis was undertaken using MetaMorph software (Universal Imaging).

RESULTS

Temporal and spatial regulation of *Mesp2* expression

To investigate the link between the segmentation clock and the spatio-temporal regulation of *Mesp2* transcription, we employed high-resolution fluorescent in situ hybridization together with immunostaining to detect active Notch (Notch intracellular domain, NICD) or Tbx6 during mouse somitogenesis. The transcriptional state of *Mesp2* in each cell was thus visualized using a mix of intronic and exonic probes and could be divided into four distinct patterns; no transcription, initiation, active state and termination (Fig. 1A-D). We also defined a Notch standard time (phase I, II or III), which was dependent on the location of the active-Notch domain in the posterior PSM and was used to monitor the segmentation clock (see Fig. S1 in the supplementary material). This double-staining system enabled us to investigate the spatio-temporal regulation of different factors during somitogenesis. We prepared a total of 18 embryos, and two sections from all 18 samples were subjected to double-staining analyses for *Mesp2* transcription and NICD or Tbx6. Each sample was sorted into phase (phase I=4, phase II=6, phase III=8) according to the Notch standard time (see Fig. S1 in the supplementary material). Since the transcriptional state of *Mesp2* changes depending on the phase, typical specimens representing each phase were selected and are shown in Figs 1 and 2. During phase II, when the oscillating Notch activity had not yet reached the anterior PSM, no *Mesp2* transcripts were detectable (Fig. 1E,F). However, once the Notch activity had reached the anterior PSM (phase III), *Mesp2* transcripts were evident in a portion of the cells within the relatively broad domain containing active-Notch-positive cells (Fig. 1G,H). Most of these cells showed nuclear dots and some began to accumulate *Mesp2* transcripts in their cytoplasm (Fig. 1K,L). In phase I, when the active-Notch domain had shrunk to a clear stripe in the anterior PSM and a new wave was present at the posterior PSM, a stronger *Mesp2* signal was observed within the active-Notch domain (Fig. 1I,J). The signals at this point could now be observed in the cytoplasm, in addition to nuclear dots in the majority of cells (Fig. 1M,N). It should also be noted that the cells exhibiting *Mesp2* transcription had a clear anterior limit and no *Mesp2* signal was detected beyond this border, even though the cells anterior to the border showed similar levels of active Notch. This indicated that Notch activity may determine the timing of *Mesp2* transcription, but not the location. We then speculated that Tbx6 might provide the spatial information required for *Mesp2* transcription.

Thus, we examined the relationship between *Mesp2* transcription and Tbx6 in the same embryos used for NICD staining, and found that the expression domain of Tbx6 had a clear anterior border, which was perfectly matched with *Mesp2* transcription in either phase III or I, when *Mesp2* transcription is detectable (Fig. 2). This indicated that Tbx6 defines the anterior limit of the *Mesp2* expression domain by serving as a potent transcriptional activator, as we have shown previously (Yasuhiko et al., 2006).

Mesp2 leads to the suppression of Tbx6 post-translationally via the ubiquitin-proteasome pathway

The next question was how is this Tbx6 anterior domain established? The answer was provided by a double staining of Mesp2 and Tbx6 proteins (see Fig. S2 in the supplementary

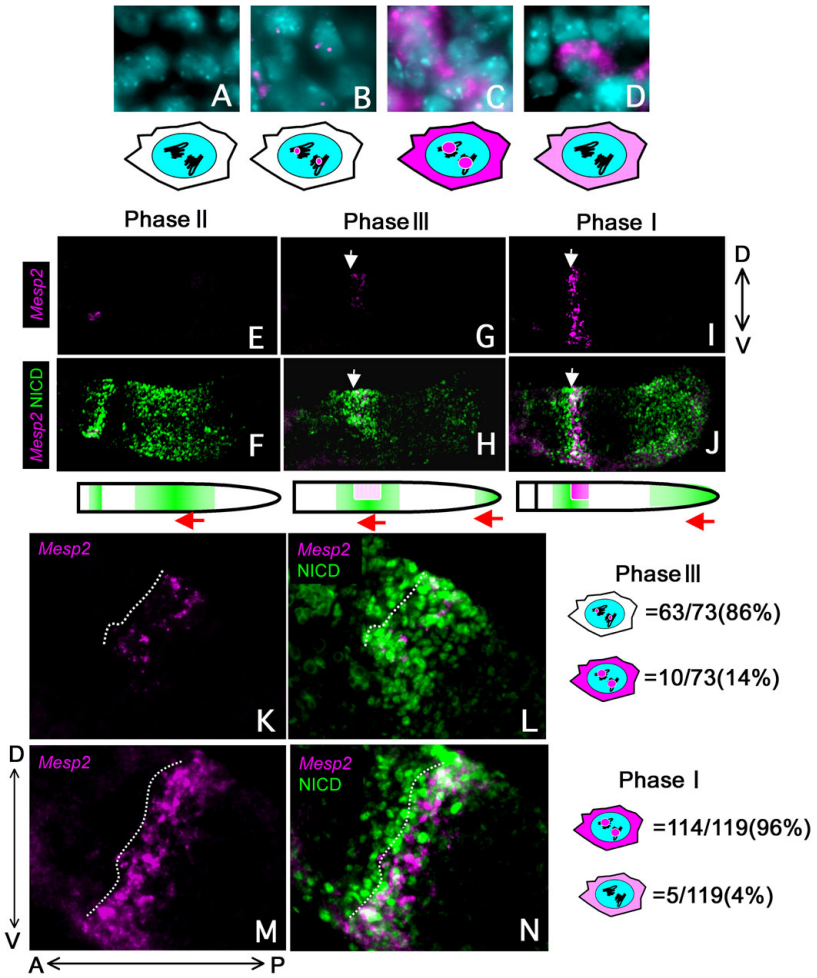

Fig. 1. The temporal regulation of *Mesp2* transcription by Notch signaling. (**A-D**) Representative *Mesp2* transcription states revealed by high-resolution in situ hybridization with combined antisense probes corresponding to an intronic region and exons of mouse *Mesp2*. (A) No transcription, (B) primary transcription, (C) active transcription and cytoplasmic accumulation of transcripts, and (D) transcriptional termination. Magenta, *Mesp2* transcripts; blue, DAPI staining. The subcellular localization of the *Mesp2* transcripts revealed by these images is depicted schematically below each panel. (**E-J**) Double staining of *Mesp2* transcripts (in situ hybridization) and Notch activity (anti-NICD antibody) during one cycle of somitogenesis. *Mesp2* transcription was not detected in phase II (E,F, *n*=5), was initiated during phase III (G,H, *n*=6), and was further upregulated in phase I (I,J, *n*=7). Arrowheads in G-J indicate anterior limits of *Mesp2* transcription. (**K-N**) Higher magnification of phase III (K,L) and phase I (M,N) images. *Mesp2* transcripts were detectable in the posterior half of the active-Notch domain with a clear anterior boundary (dotted lines). The actual numbers of cells showing different subcellular localization of *Mesp2* transcripts are shown on the right of the panels for phase III and I.

material). Differing from the *Mesp2* transcript profile (Fig. 2), the expression domain of the Mesp2 protein was completely segregated from that of the Tbx6 protein in phase-II embryos in which *Mesp2* transcription had ceased (see Fig. S2 in the supplementary material). This suggested that once *Mesp2* expression is activated by Tbx6, the Mesp2 protein then induces the suppression of Tbx6 protein expression in a cell-autonomous manner. This possibility was supported by our analysis of *Mesp2*-null embryos, in which Tbx6 protein expression was expanded into the anterior somitic region (Fig. 3A,B,E). Intriguingly, however, the *Tbx6* transcripts detected by in situ hybridization did not extend anteriorly in the *Mesp2*-null embryo (Fig. 3D), and instead displayed a pattern that was similar to that of the wild type (Fig. 3C). These data indicate that Mesp2 is involved in the post-translational regulation of the Tbx6 protein, which is stabilized in the absence of Mesp2 for at least 12 hours, by our estimation (Fig. 3E). These results also indicate that Tbx6 protein is rapidly degraded downstream of Mesp2. To identify proteases responsible for Tbx6 protein degradation, we tested two types of protease inhibitors: PMSF, a serine protease inhibitor, and MG132, a proteasome inhibitor. The caudal part of an embryo was bisected, and one half was treated with inhibitors for 2 hours while the other half was treated with DMSO (control). After treatment, Tbx6 protein was detected by antibody staining. The proteasome inhibitor, MG132, stabilized Tbx6 protein (Fig. 3F), whereas PMSF did not (Fig. 3G). These results suggest that Tbx6 protein is rapidly degraded via a ubiquitin-mediated proteasome pathway downstream of Mesp2. The stabilized Tbx6 proteins would then be responsible for the *Mesp2*-null mouse phenotype, in which expression of both *Dll1* and *Mesp2* is expanded [previously revealed by our analysis of a *Mesp2-lacZ* knock-in embryo (Takahashi et al., 2000)], as *Dll1* transcription has been shown to be activated by Tbx6 (Galceran et al., 2004; Hofmann et al., 2004; White and Chapman, 2005).

The above results indicate that interactions between Mesp2, Tbx6 and Notch are crucial for the translation of the temporal information supplied by Notch activity into spatial patterning. To elucidate the dynamic regulatory network underlying this process in more detail, we investigated the spatio-temporal relationships between these three factors during somitogenesis. To this end, a total of 20 embryos were prepared at E10.5 and three sections from each were subjected to double-immunostaining analyses for Mesp2 and NICD, Mesp2 and Tbx6, or NICD and Tbx6. These experiments enabled us to determine the relationship between each pair of factors at a fixed time point. Staining results were arranged according to the Notch standard time (see Fig. S1 in the supplementary material), and the temporal and spatial dynamics of the expression patterns were revealed. We observed distinct patterns that were dependent on the segmentation stages. In phase III, once Notch activity had reached the anterior PSM and during which time *Mesp2* transcription had been initiated (Fig. 1G), Mesp2 proteins became detectable in the posterior part of the NICD domain in a similar manner to *Mesp2* transcripts (Fig. 3H). This region also corresponds to the anterior limit of the Tbx6-expressing domain (Fig. 3I). During phase I, when

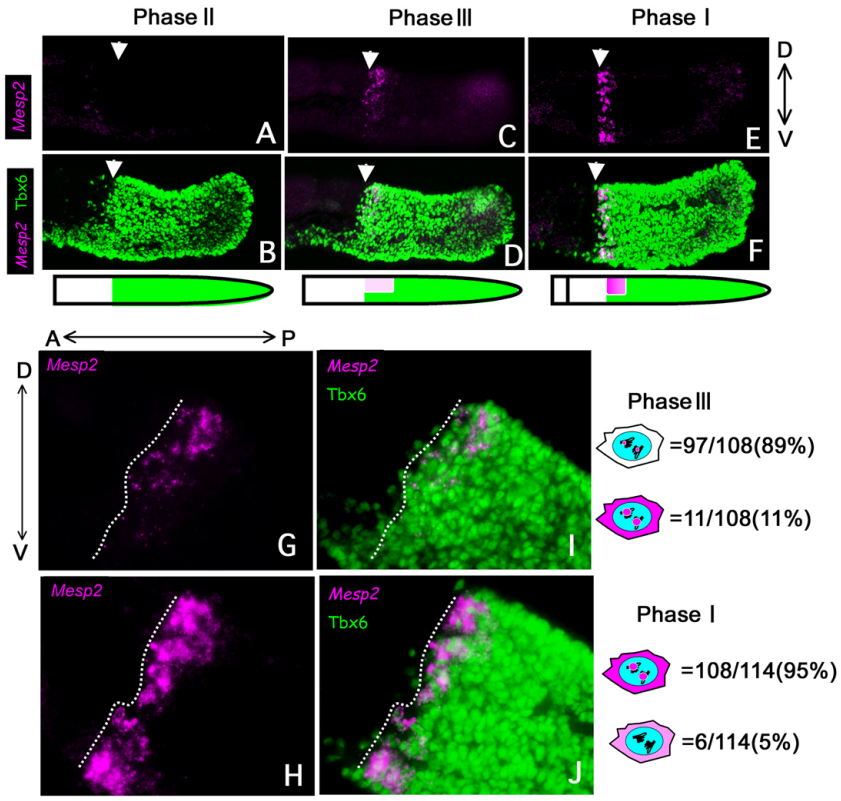

Fig. 2. *Mesp2* transcription occurs at the anterior end of the Tbx6 expression domain. (**A-J**) Spatio-temporal changes in the *Mesp2* transcription pattern during somitogenesis. Double staining of *Mesp2* and NICD (see Fig. 1E-N) or of *Mesp2* and Tbx6 (A-F) was conducted using a single mouse embryo for each phase. (A,B) Phase II, (C,D) phase III and (E,F) phase I. The staining patterns for B,D,F are also shown schematically. (G,H) Magnified images of C,D. (I,J) Magnified images of E,F. The transcriptional states in I and J were roughly estimated using the subcellular localization pattern of the *Mesp2* transcripts and are shown in the right-hand panel.

Mesp2 transcription is robust (Fig. 1I), the Mesp2 expression domain overlapped with those of NICD and Tbx6, and Tbx6 protein expression began to be repressed (Fig. 3J,K). During phase II, when *Mesp2* is no longer transcribed (Fig. 1E) and the next wave has just reached the anterior PSM, there was complete segregation of these three signals and, thus, boundaries formed between NICD and Mesp2 (Fig. 3L), thereby demarcating the segmental border as previously described (Morimoto et al., 2005). Boundaries also formed between the Mesp2 and Tbx6 expression domains (Fig. 3M), generating the next Mesp2 anterior limit and, thus, the next segmental border.

Initiation of Notch signal oscillation correlates with the onset of *Mesp2* transcription

The next question was when and how is the cycle of these three factors established? To address this, we focused on early stage embryos prior to segmented somite formation at ~E7.0-7.5. We found two distinct patterns for Tbx6 expression in E7.0-7.5 embryos that do not have segmented somites. In earlier stage embryos (E.7.0, Fig. 4A), Tbx6 expression was graded without a clear anterior limit (data not shown). These embryos never had Mesp2 expression or Notch signal oscillation, although both NICD (the weak signal in the mesoderm) and Tbx6 expression could be detected (Fig. 4A-C). Similarly, in E7.0 embryos, *Hes7* and *Lfng*, which are essential for Notch signal oscillation, were weakly expressed, but did not show clear wave-like patterns (Fig. 4D-I). These results suggested that the low-level expression of *Hes7* and *Lfng* might not be enough to generate Notch signal oscillation. The other pattern observed in slightly later stage embryos (E7.5, Fig. 4J) was characterized by a clear anterior boundary for the Tbx6 protein and a Mesp2 expression stripe just anterior to the Tbx6 domain (Fig. 4K,L). Intriguingly, an oscillatory pattern of Notch activity was detected (Fig. 4M) and the spatial patterns of the three factors (Fig. 4J-N) were similar to those of later stage embryos as shown in Fig. 3I-L. The clear difference between the two groups of embryos was the absence or presence of Notch signal oscillation, indicating that the commencement of this oscillation may trigger the initial activation of *Mesp2* transcription.

FGF signaling together with Wnt signaling gradients may determine the *Mesp2* expression domain

A remaining question concerned the mechanisms that define the posterior border of *Mesp2* expression: what determines the width of a single somite and why is *Mesp2* expression suppressed in the posterior PSM in spite of the presence of Tbx6, an activator of *Mesp2*? It has been suggested that the *Mesp2* expression domain is defined by a so-called determination front, which is proposed to be defined by an antagonistic gradient of RA and FGF signaling (Delfini et al., 2005; Moreno and Kintner, 2004; Wahl et al., 2007).

We examined the expression pattern of *Dusp4*, an FGF signaling target gene that shows an oscillation pattern in the posterior PSM (Niwa et al., 2007). Interestingly, the anterior limit of the *Dusp4* expression domain corresponded to the posterior limit of *Mesp2* (Fig. 5A-C), which supports the possibility that FGF signaling determines the posterior border of the *Mesp2* expression domain by negatively regulating *Mesp2* expression. The *Dusp4* expression pattern was unchanged and did not expand anteriorly in the absence of Mesp2 (Fig. 5D,E), which indicates that FGF signaling works upstream of Mesp2 function.

We next examined whether the *Mesp2* expression domain was altered by the lack of FGF signaling. The PSM-specific *Fgfr1* knockout (*Fgfr1*-cKO) results in a gradual loss of PSM supply and the truncation of the tailbud (Niwa et al., 2007; Wahl et al., 2007). In such mutant embryos, a posterior shift in the *Mesp2* expression

domain was consistently observed (Fig. 5F and data not shown). However, *Mesp2* expression did not completely regress to the posterior end of the PSM, indicating the presence of other factors responsible for positioning the determination front (see below). Using specimens with less severe truncations of the PSM, we examined the relationship among Mesp2, Notch and Tbx6 by immunohistochemistry (Fig. 5I-L). Tbx6 expression was observed in the PSM without a clear anterior border, and this was accompanied by a slight anterior expansion of Mesp2 expression in the *Fgfr1*-cKO embryo (Fig. 5J). Lower, but continuous, Notch activity was observed in the posterior PSM without apparent oscillation in the *Fgfr1*-cKO embryo, and a higher level of Notch activity almost merged with the Mesp2 expression domain (Fig. 5L), suggesting that the posterior shift of the active-Notch domain caused by the lack of FGF signaling is responsible for the posterior shift of Mesp2. To further examine the involvement of FGF signal in *Mesp2* expression, we cultured caudal portions of E10 embryos with the FGF inhibitor SU5402 or with DMSO as control for 6 hours. Similar to what was observed for the *Fgfr1*-cKO embryo, a posterior shift in the *Mesp2* expression domain was observed in SU5402-treated embryos (Fig. 5G). To examine the effects of FGF signals in the same embryo, bisected caudal portions of E10 embryos were treated with SU5402 or DMSO for 2 hours. In the presence of SU5402, the *Mesp2* expression domain was shifted posteriorly by a distance of approximately one-half to one-somite as compared with the control (Fig. 5H), confirming that FGF signaling is involved in the positioning of the determination front.

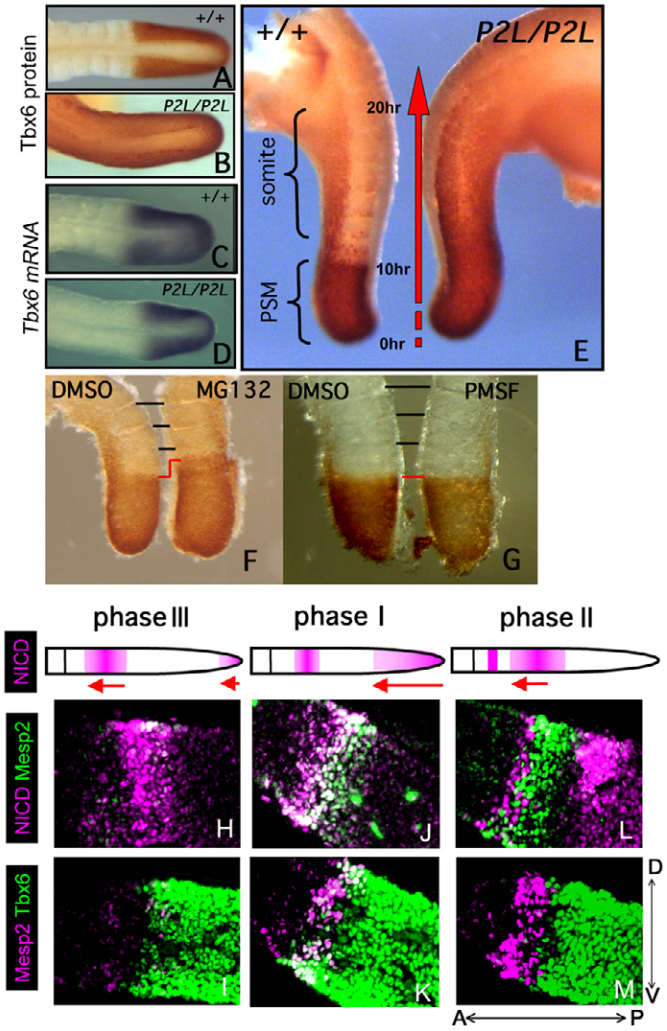

Fig. 3. Mesp2 induces the degradation of Tbx6 via a ubiquitin-proteasome pathway. (**A-D**) Comparison of the expression patterns for Tbx6 protein (A,B) and mRNA (C,D) between wild-type (+/+) and *Mesp2*-null (P2L/P2L) mice. Dorsal views, anterior to the left. *n*=4 (A), *n*=3 (B), *n*=3 (C), *n*=4 (D). (**E**) The stability of Tbx6 was compared in embryonic tails with or without Mesp2. The time was estimated by the number of somites formed in the wild-type embryo. (**F**,**G**) Caudal portions of E10 embryos were bisected and the left halves treated with DMSO (control), while the right halves were treated with MG132 (F, *n*=10) or PMSF (G, *n*=3) and immunostained for Tbx6. (**H-M**) Double-immunostaining patterns representative of the relationships between Mesp2, Tbx6 and Notch during somitogenesis. The stained sections shown in the vertical rows are derived from a single embryo. A schematic of the Notch activity pattern used to assign the phase of the embryo is shown in the top panels; phase III (*n*=6), phase II (*n*=9), phase I (*n*=5). The proteins being detected are indicated in the left panels. A-P, anterior-posterior; D-V, dorsal-ventral.

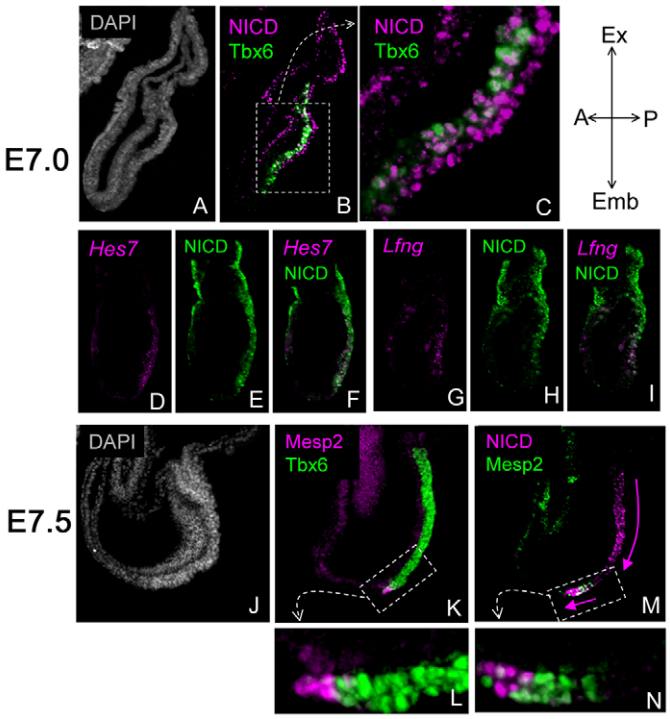

Fig. 4. Initiation of Notch signal oscillation correlates with the onset of *Mesp2* transcription. (**A-I**) Sections of early stage mouse embryos (~E7.0) were analyzed by double immunostaining. (A-C) The embryos were stained with DAPI (A), and with antibodies against NICD and Tbx6 (B,C). A higher magnification image of B is shown in C. These embryos showed weak NICD activity without oscillation, and Tbx6 expression (*n*=13). (D-I) Sections were also subjected to double staining for *Hes7* mRNA and NICD (D-F), and *Lfng* mRNA and NICD (G-I). *Hes7* and *Lfng* mRNAs were weakly expressed, but did not show clear wave-like patterns (*n*=10). (**J-N**) Sections of late-streak stage embryos just prior to somite formation (~E7.5) were stained with DAPI to show the embryonic structure (J), and double stained for Tbx6 and Mesp2 (K,L), or Mesp2 and NICD (M,N). Higher magnification images for K and M are shown in L and N, respectively. An oscillatory pattern of Notch activity was detected and the spatial patterns of the three factors were similar to those of later stage embryos (*n*=12). Ex, extraembryonic region; Emb, embryonic region.

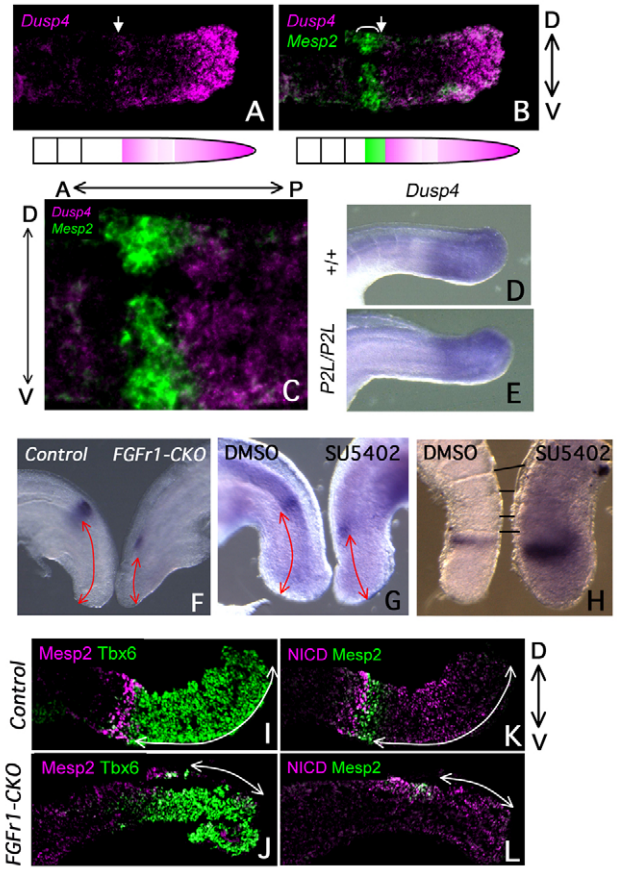

Fig. 5. Effects of the FGF signaling pathway on the regulation of *Mesp2* expression. (**A-C**) The spatial relationship between *Mesp2* (using mRNA probe) and *Dusp4* was examined by double in situ hybridization. The posterior border of the *Mesp2* expression domain (round bracket in B) coincides with the anterior limit of the *Dusp4* expression domain (border indicated by arrow in A,B). The stage of this embryo was assigned as phase I. A higher magnification image of B is shown in C. (**D**,**E**) *Dusp4* expression revealed by whole-mount in situ hybridization in wild-type (D, *n*=4) and *Mesp2*-null (*P2L/P2L*; E, *n*=2) embryos. (**F**) An analysis of PSM-specific *Fgfr1* knockout (cKO) mice. Whole-mount in situ hybridization revealed a posterior shift of the *Mesp2* expression domain in the *Fgfr1*-cKO embryo (*n*=8). (**G**) Caudal portions of E10.5 embryos were treated with FGF inhibitor (SU5402) or DMSO (control) for 6 hours. A posterior shift of the *Mesp2* expression domain was observed in the embryos treated with SU5402 (5 out of 6 embryos). (**H**) Caudal portions of E10 embryos were bisected and the left halves were treated with DMSO (control), while the right halves were treated with SU5402. A posterior shift of the *Mesp2* expression domain was observed in 10 out of 13 SU5402-treated embryos tested. (**I-L**) Double immunostaining of sections was employed to examine Tbx6 and Mesp2 (I,J) or Mesp2 and NICD (K,L) expression in wild-type control (I,K) and *Fgfr1*-cKO (J,L) embryos.

Another possible factor involved in positioning the *Mesp2* expression domain is Wnt, as it was recently shown that the ectopic activation of β-catenin in the PSM leads to an anterior shift of the *Mesp2* expression domain (Aulehla et al., 2007). We examined the expression of mesogenin 1 (*Msgn1*), one of the downstream targets of Tbx6 and Wnt signaling (Wittler et al., 2007). In the wild-type embryo, *Msgn1* was expressed in the posterior PSM but declined posterior to the *Dusp4* domain, thereby forming a gap between the *Mesp2* and *Msgn1* expression domains (see Fig. S3A-C in the supplementary material). As with *Dusp4*, the expression pattern of *Msgn1* was unchanged in the *Mesp2*-null embryo (see Fig. S3D,E in the supplementary material). Thus, Wnt signaling also functions upstream of Mesp2, but is unlikely to determine the posterior limit of the *Mesp2* expression domain. Nevertheless, Wnt could be involved in the suppression of *Mesp2* in the posterior PSM because Wnt signaling is known to be maintained in the absence of FGF signaling (Niwa et al., 2007; Wahl et al., 2007).

DISCUSSION

In these studies, we have used sensitive methods of fluorescent in situ hybridization in conjunction with immunofluorescent staining to visualize dynamic changes of gene activities in the determination front, at which the temporal information supplied by the segmentation clock is translated into spatial pattern. Our current model is schematically summarized in Fig. 6. We propose that the periodic activation of *Mesp2* in the anterior PSM is achieved by the cooperative function of two positive factors: Tbx6 (spatial factor) and Notch (temporal factor). This, together with the negative effect of positional information provided from the posterior end by pathways such as FGF and Wnt signaling, and the reciprocal regulation of the determination front by the negative-feedback function of Mesp2, constitute a key mechanism for the continuous generation of somites in the anterior PSM.

Mesp2 post-translationally suppresses Tbx6 protein expression

The most intriguing finding of our current study is the suppression of Tbx6 via rapid degradation mediated by the ubiquitin-proteasome pathway under the control of Mesp2. Previously, we have shown that Mesp2 establishes the RC polarity within a somite by suppressing *Dll1* expression (Takahashi et al., 2000). However, the real target of Mesp2 function was found to be Tbx6, as *Dll1* is a downstream target of Tbx6 (Galceran et al., 2004; Hofmann et al., 2004; White and Chapman, 2005). In the absence of Mesp2, Tbx6 is expanded anteriorly, which accounts for the anterior expansion of *Dll1*, and this leads to somite caudalization. In addition, our model also explains how the RC polarity is established during normal somitogenesis. This process is shown in Fig. S4 in the supplementary material: during phase I-II, Mesp2 is activated by a wave of Notch activity and suppresses *Dll1* expression within one somite length via the downregulation of Tbx6 (see Fig. S4A-D). In phase III, the next Notch wave is initiated in this region, which includes the presumptive caudal compartment of the somite that has already experienced Mesp2 expression and the next presumptive somite (see Fig. S4E,F). Finally, the caudal *Dll1* stripe is generated by Psen1-dependent Notch activation, which is independent of Tbx6 (see Fig. S4G) (Takahashi et al., 2000).

The periodicity of mouse somitogenesis has been explained by the nature of the segmentation clock. However, the oscillations themselves do not form a segmental boundary. We speculate that Mesp2 serves as the final output signal of this clock network and that it translates the temporal information required to generate correctly segmented paraxial mesoderm. We have also elucidated the mechanism underlying the activation of periodic *Mesp2* transcription in the anterior PSM. *Mesp2* expression is activated by Tbx6-dependent Notch activity, but this then leads to destabilization of Tbx6 protein by the ubiquitin-proteasome pathway. The negative regulation of Tbx6 is essential for the formation of the next anterior border of the *Mesp2* expression domain, which also marks the next segmental border. However, the direct target of Mesp2, which leads to the rapid degradation of Tbx6, is currently unknown. Recently, several groups

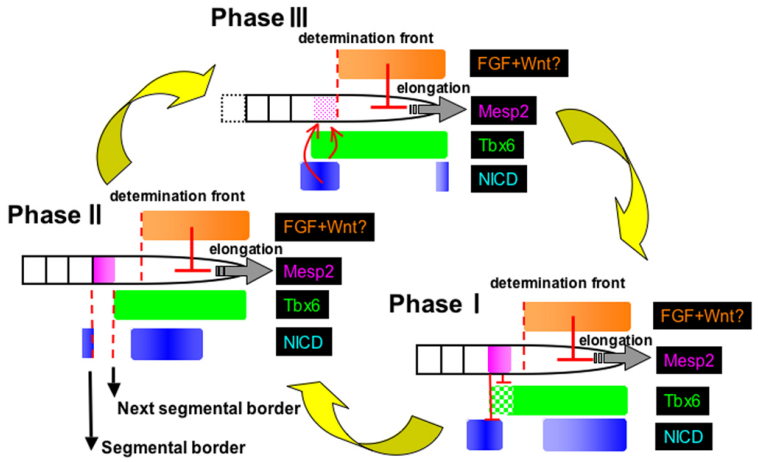

Fig. 6. A model for periodic somitogenesis in the mouse. Schematic representation of the temporal and spatial changes in the expression patterns and relationships among Mesp2 (pink), Tbx6 (green), NICD (blue) and FGF signaling (orange) during a single cycle of somitogenesis. The FGF signal is provided from the PSM with a posterior-to-anterior gradient. The expected threshold in the activity defines the determination front that corresponds to the posterior limit of the *Mesp2* expression domain. In phase III, Notch activity reaches the anterior PSM, where *Mesp2* transcription has been initiated in the cells with Tbx6 expression and lacking negative effectors such as FGF and Wnt signaling. In phase I, Mesp2 protein accumulates and suppresses NICD by activating Lfng, and also suppresses Tbx6 protein by promoting its rapid degradation via the ubiquitin-proteasome pathway. In phase II, when the next wave of Notch activity has just reached the anterior PSM region, the three signals (NICD, Mesp2 and Tbx6) show complete segregation, thus establishing a boundary between NICD and Mesp2 that demarcates the segmental border, and a boundary between Mesp2 and Tbx6 that demarcates the next Mesp2 anterior limit and, thus, the next segmental border.

including us reported Ripply family proteins as potential negative regulators of Mesp family gene expression (Chan et al., 2007; Kawamura et al., 2005; Kondow et al., 2007; Morimoto et al., 2007). Mouse *Ripply2*-null embryos show prolonged expression of *Mesp2* (Morimoto et al., 2007). Interestingly, in *Xenopus laevis*, Tbx6-dependent transcription of *Thylacine 1*, a homolog of mouse *Mesp2*, was suppressed by Bowline, a Ripply family protein (Kondow et al., 2007). Furthermore, Tbx6 and Mesp2 synergistically activate *Ripply2* expression in the mouse (Dunty et al., 2008; Hitachi et al., 2007). These results suggest that *Ripply2* is activated by Mesp2 and Tbx6, but that it in turn suppresses the transcriptional activity of Tbx6 at the termination step of somite segmentation. However, expression of both *Dll1* and *Mesp2*, which are direct targets of Tbx6, was markedly expanded to the anterior somitic region in the *Mesp2*-null mouse, whereas *Mesp2* expression was only slightly prolonged and *Dll1* expression was not expanded but rather suppressed in the *Ripply2*-null mouse (Morimoto et al., 2007). Thus, suppression of Tbx6 activity downstream of Mesp2 cannot be solely due to Ripply2. Importantly, whereas the Tbx6 protein expression domain was expanded anteriorly in the *Mesp2*-null embryo, it was not altered in the *Ripply2*-null embryo (our unpublished data), and Ripply family members are not known to be involved in protein degradation, indicating that Mesp2 suppresses Tbx6 protein expression independently of Ripply2. Thus, downstream of Mesp2, Tbx6 appears to be inactivated by two independent pathways: a Ripply2-dependent pathway, which leads to the suppression of Tbx6 activity (*Xenopus* studies), and a Ripply2-independent/Mesp-dependent pathway, which leads to the degradation of Tbx6 protein (this study). We speculate that these pathways are essential for suppressing Tbx6 activity completely and for allowing periodic formation of somites. The identification of the E3 ubiquitin ligase specific to Tbx6, the identification of the direct targets of Mesp2 and further clarification of the genetic network in which this transcription factor exerts its functional role will be required to resolve this complex and sophisticated segmentation program.

An additional factor(s) is required for the suppression of *Mesp2* in the posterior PSM

In this study, we demonstrate that FGF signaling together with Wnt signaling gradients contribute to the *Mesp2* expression domain. However, the mechanism involved in the negative regulation of *Mesp2* in the posterior PSM is not clear. FGF signaling might account for the correct positioning of the determination front. However, the direct link with *Mesp2* expression was not revealed by the loss-of-function study of FGF signaling. Another candidate, Wnt signaling, appears to function upstream of FGF signaling (Aulehla et al., 2007; Dunty et al., 2008), and *Mesp2* expression is essentially lost in the absence of Wnt signaling (Dunty et al., 2008). However, *Mesp2* expression is retained in the presumptive determination front even in the absence of FGF signaling when ectopic Wnt signaling is maintained in the PSM (Aulehla et al., 2007), which indicates the lack of a simple epistatic relationship between FGF and Wnt signaling in the PSM. Another difficulty resides in the fact that these signaling pathways are also required for the formation of paraxial mesoderm (Aulehla et al., 2007; Dunty et al., 2008; Niwa et al., 2007; Wahl et al., 2007). Therefore, loss-of-function and gain-of-function studies are complicated by their affects on the generation of paraxial mesoderm and so might occasionally provide misleading information. We believe that our current comprehensive analyses of normal somitogenesis using wild-type embryos provide valuable information to be challenged by different experimental approaches by ourselves and others. Hence, it is probable that other negative effectors besides FGF and Wnt signals exist in the posterior PSM and regulate *Mesp2* expression.

What triggers the onset of Notch oscillation?

We demonstrated that the initiation of Notch signal oscillation correlated with the onset of *Mesp2* transcription. In the chick embryo, the onset of dynamic expression of the cyclic genes *Chairy2* and *Lfng* correlates with ingression of the paraxial mesoderm territory from the epiblast into the primitive streak,

although the first two pulses of cyclic gene expression showing longer periods are associated with head mesoderm formation and not somite formation (Jouve et al., 2002). In our study using E7.0 mouse embryos prior to somite formation, we observed only weak and uniform signals for both Notch activity and *Hes7* and *Lfng* expression patterns. We do not exclude the possibility that the cyclic pattern might exist in the mouse embryo at this stage, with a longer time phase like that seen in the chick. However, we did not observe clear Notch signal oscillation until slightly later, at E7.5, and this showed a strong correlation with the onset of *Mesp2* transcription. Therefore, we speculate that although Hes7 and Lfng are expressed earlier, either the presence of these negative regulatory signals, or their low expression levels, is not sufficient to create a cyclic pattern of gene expression. The regulatory mechanisms leading to the initiation of Notch signal oscillation and *Mesp2* transcription remain elusive.

We thank Chu-Xia Deng (National Institutes of Health, USA) for providing floxed *Fgfr1* mice and Aya Satoh (National Institute of Genetics, Japan) for animal care. This work was supported in part by Grants-in-Aid for Scientific Research on Priority Areas, Dynamics of Extracellular Environments, and for the National BioResource Project from the Ministry of Education, Culture, Sports, Science and Technology, Japan.

Supplementary material

Supplementary material for this article is available at http://dev.biologists.org/cgi/content/full/135/15/2555/DC1

References

Aulehla, A., Wiegraebe, W., Baubet, V., Wahl, M. B., Deng, C., Taketo, M., Lewandoski, M. and Pourquie, O. (2007). A beta-catenin gradient links the clock and wavefront systems in mouse embryo segmentation. *Nat. Cell Biol.* **10**, 181-193.

Bessho, Y., Sakata, R., Komatsu, S., Shiota, K., Yamada, S. and Kageyama, R. (2001). Dynamic expression and essential functions of Hes7 in somite segmentation. *Genes Dev.* **15**, 2642-2647.

Bessho, Y., Hirata, H., Masamizu, Y. and Kageyama, R. (2003). Periodic repression by the bHLH factor Hes7 is an essential mechanism for the somite segmentation clock. *Genes Dev.* **17**, 1451-1456.

Chan, T., Kondow, A., Hosoya, A., Hitachi, K., Yukita, A., Okabayashi, K., Nakamura, H., Ozawa, H., Kiyonari, H., Michiue, T. et al. (2007). Ripply2 is essential for precise somite formation during mouse early development. *FEBS Lett.* **581**, 2691-2696.

Delfini, M. C., Dubrulle, J., Malapert, P., Chal, J. and Pourquie, O. (2005). Control of the segmentation process by graded MAPK/ERK activation in the chick embryo. *Proc. Natl. Acad. Sci. USA* **102**, 11343-11348.

Dunty, W. C., Jr, Biris, K. K., Chalamalasetty, R. B., Taketo, M. M., Lewandoski, M. and Yamaguchi, T. P. (2008). Wnt3a/β-catenin signaling controls posterior body development by coordinating mesoderm formation and segmentation. *Development* **135**, 85-94.

Galceran, J., Sustmann, C., Hsu, S. C., Folberth, S. and Grosschedl, R. (2004). LEF1-mediated regulation of Delta-like1 links Wnt and Notch signaling in somitogenesis. *Genes Dev.* **18**, 2718-2723.

Hitachi, K., Kondow, A., Danno, H., Inui, M., Uchiyama, H. and Asashima, M. (2007). Tbx6, Thylacine1, and E47 synergistically activate bowline expression in Xenopus somitogenesis. *Dev. Biol.* **313**, 816-828.

Hofmann, M., Schuster-Gossler, K., Watabe-Rudolph, M., Aulehla, A., Herrmann, B. G. and Gossler, A. (2004). WNT signaling, in synergy with T/TBX6, controls Notch signaling by regulating Dll1 expression in the presomitic mesoderm of mouse embryos. *Genes Dev.* **18**, 2712-2717.

Huppert, S. S., Ilagan, M. X., De Strooper, B. and Kopan, R. (2005). Analysis of Notch function in presomitic mesoderm suggests a gamma-secretase-independent role for presenilins in somite differentiation. *Dev. Cell* **8**, 677-688.

Jouve, C., Iimura, T. and Pourquie, O. (2002). Onset of the segmentation clock in the chick embryo: evidence for oscillations in the somite precursors in the primitive streak. *Development* **129**, 1107-1117.

Kawamura, A., Koshida, S., Hijikata, H., Ohbayashi, A., Kondoh, H. and Takada, S. (2005). Groucho-associated transcriptional repressor ripply1 is required for proper transition from the presomitic mesoderm to somites. *Dev. Cell* **9**, 735-744.

Kondow, A., Hitachi, K., Okabayashi, K., Hayashi, N. and Asashima, M. (2007). Bowline mediates association of the transcriptional corepressor XGrg-4 with Tbx6 during somitogenesis in Xenopus. *Biochem. Biophys. Res. Commun.* **359**, 959-964.

Moreno, T. A. and Kintner, C. (2004). Regulation of segmental patterning by retinoic acid signaling during Xenopus somitogenesis. *Dev. Cell* **6**, 205-218.

Morimoto, M., Takahashi, Y., Endo, M. and Saga, Y. (2005). The Mesp2 transcription factor establishes segmental borders by suppressing Notch activity. *Nature* **435**, 354-359.

Morimoto, M., Sasaki, N., Oginuma, M., Kiso, M., Igarashi, K., Aizaki, K., Kanno, J. and Saga, Y. (2007). The negative regulation of Mesp2 by mouse Ripply2 is required to establish the rostro-caudal patterning within a somite. *Development* **134**, 1561-1569.

Niwa, Y., Masamizu, Y., Liu, T., Nakayama, R., Deng, C. X. and Kageyama, R. (2007). The initiation and propagation of Hes7 oscillation are cooperatively regulated by Fgf and notch signaling in the somite segmentation clock. *Dev. Cell* **13**, 298-304.

Takahashi, Y., Koizumi, K., Takagi, A., Kitajima, S., Inoue, T., Koseki, H. and Saga, Y. (2000). Mesp2 initiates somite segmentation through the Notch signalling pathway. *Nat. Genet.* **25**, 390-396.

Wahl, M. B., Deng, C., Lewandoski, M. and Pourquie, O. (2007). FGF signaling acts upstream of the NOTCH and WNT signaling pathways to control segmentation clock oscillations in mouse somitogenesis. *Development* **134**, 4033-4041.

White, P. H. and Chapman, D. L. (2005). Dll1 is a downstream target of Tbx6 in the paraxial mesoderm. *Genesis* **42**, 193-202.

Wittler, L., Shin, E. H., Grote, P., Kispert, A., Beckers, A., Gossler, A., Werber, M. and Herrmann, B. G. (2007). Expression of Msgn1 in the presomitic mesoderm is controlled by synergism of WNT signalling and Tbx6. *EMBO Rep.* **8**, 784-789.

Xu, X., Qiao, W., Li, C. and Deng, C. X. (2002). Generation of Fgfr1 conditional knockout mice. *Genesis* **32**, 85-86.

Yasuhiko, Y., Haraguchi, S., Kitajima, S., Takahashi, Y., Kanno, J. and Saga, Y. (2006). Tbx6-mediated Notch signaling controls somite-specific Mesp2 expression. *Proc. Natl. Acad. Sci. USA* **103**, 3651-3656.